Improving oncolytic viral therapy for glioma

Idema, S.

2011

document version
Publisher's PDF, also known as Version of record

CHAPTER 5

ANATOMICAL DIFFERENCES DETERMINE DISTRIBUTION OF ADENOVIRUS AFTER CONVECTION-ENHANCED DELIVERY TO THE RAT BRAIN

Sander Idema, Viola Caretti, Martine L.M. Lamfers, Victor W. van Beusechem, David P. Noske, W. Peter Vandertop, Clemens M.F. Dirven

Manuscript in preparation

ABSTRACT

Convection-enhanced delivery (CED) of adenoviruses offers the potential of widespread virus distribution in the brain. In CED, the volume of distribution (Vd) should be related to the volume of infusion (Vi) and not to dose, but when using adenoviruses contrasting results have been reported. As the characteristics of the infused tissue can affect convective delivery, this study was performed to determine the effects of the gray and white matter on CED of adenoviruses and similar sized super paramagnetic iron oxide nanoparticles (SPIO). We convected AdGFP, an adenovirus vector expressing Green Fluorescent Protein, a virus sized SPIO or trypan blue in the gray and white matter of the striatum and external capsule of Wistar rats and towards orthotopic infiltrative brain tumors. The resulting Vds were compared to Vi and transgene expression to SPIO distribution.

Results show that in the striatum Vd is not determined by the Vi but by the infused virus dose, suggesting diffusion, active transport or receptor saturation rather than convection. Distribution of virus and SPIO in the white matter is partly volume dependent, which is probably caused by preferential fluid pathways from the external capsule to the surrounding gray matter, as demonstrated by co-infusing trypan blue. Distant tumors were reached using the white matter tracts but tumor penetration was limited.

CED of adenoviruses in the rat brain and towards infiltrative tumors is feasible when regional anatomical differences are taken into account while SPIO infusion could be considered to validate proper catheter positioning and predict adenoviral distribution.

INTRODUCTION

Convection-enhanced delivery (CED) is a novel way to circumvent the Blood-Brain Barrier (BBB) in the treatment of diseases of the brain including gliomas and neurodegenerative diseases [1-4]. Direct infusion of therapeutic agents into the interstitial space has the potential to achieve a widespread local distribution of the agent while minimising systemic degradation and toxicity. Ideally, the distribution volume (Vd) following CED is dependent on the infusion volume (Vi). Recent clinical trials have shown the safety of CED in the treatment of Glioblastoma Multiforme (GBM) [5-7]. In addition, these trials have illustrated some of the technical challenges of CED and the need to monitor the process of convection to prevent toxicity on one hand and frank ineffectiveness due to limited convection on the other [8]. Adenoviral vectors or conditionally replicating adenoviruses (CRAds) have been used preclinically and clinically in a variety of intracranial diseases [9, 10]. After intravascular, intrathecal or intracerebral delivery, adenovirus distribution and therapeutic effects are limited due to the presence of the BBB, limited diffusion of injected viral particles or elimination by the activated immune system [11-13]. As CED relies on bulk flow instead of diffusion, it represents a promising method to deliver adenoviruses to the brain. Thus far, controversy exists whether adenoviruses are suitable agents for CED [14, 15]. The size of the adenoviral particle (70-90nm) is considered to be an important determinant of its distribution, although other factors have been suggested as well [14, 16].

Ideally, CED of adenovirus should be monitored by either directly visualizing the viral particle, or by infusion of a surrogate marker with similar CED-characteristics. To determine whether regional anatomical differences influence adenoviral distribution we convected an adenoviral vector expressing Green Fluorescent Protein (GFP) into the gray and white matter of the rat brain. Additionally, we infused Superparamagnetic Iron Oxide Nanoparticles (SPIOs) as a surrogate tracer to predict the volume of adenovirus distribution after CED, while proper infusate delivery was confirmed by co-infusion of trypan blue. Finally, infiltrative tumors were targeted using white matter tracts as the delivery route for adenoviruses and SPIO.

MATERIALS & METHODS

Tumor cells and Adenoviral vectors

U-251MG malignant glioma cells and C6 rat glioma cells were obtained from the ATCC (Manassas, VA) and maintained in DMEM containing 10% Fetal Calf Serum (Gibco BRL Life Technologies, Paisley, UK).

AdGFP and AdCMVLacZ are replication-deficient adenoviral vectors carrying an expression cassette for enhanced green fluorescent protein and the Escherichia coli β-galactosidase gene respectively under control of the human CMV promoter

in the deleted E1 region of the adenoviral backbone and have been described before [17, 18]. Vectors were propagated on 293 cells and purified by CsCl gradient according to standard techniques. AdΔ24-CMV-GFP was constructed by inserting a GFP expression cassette under control of the CMV promoter in the deleted E3 region of AdΔ24,[19] which carries a 24bp deletion in the E1a region, limiting replication to cells with a dysfunctional Rb pathway [20]. AdΔ24-CMV-GFP was plaque purified and propagated on A549 cells. Viral titers in infectious units (iu) were determined by limiting dilution assay on 911 cells by hexon protein staining 48 hours after infection.

Infection efficiency assay

U-251MG cells were plated in 96-well plates at 10,000 cells per well. The next day, cells were washed in PBS and AdGFP was added at 5 iu/cell for 30 minutes with human serum albumin (HSA, Cealb, Sanquin, Amsterdam, the Netherlands) diluted in serum-free DMEM. HSA concentrations were 0% (control), 0.04% (approximate CSF albumin concentration) 0.4% (approximate concentration in cell culture medium containing 10% FCS) and 4% (albumin concentration in normal human serum). After this period, cells were washed three times in PBS, and fresh complete culture medium was added. GFP expression was assessed after 36 hours by FACS analysis. The infection efficiency of C6 cells was assessed by adding either AdGFP or AdΔ24-CMV-GFP for one hour at 100 iu/cell and determining the percentage of cells expressing GFP after 36 hours.

Infusion system

Pressure from a syringe pump (PHD 2000, Harvard Apparatus Inc., Holliston, MA) was transmitted to a syringe by way of a non-compliant and zero dead volume pressure transduction system described by Lonser et al [21]. Infusate was loaded into a 10µl Hamilton gastight syringe (RN1701, Hamilton Comp., Reno, NV) attached at one end to the pressure transduction system and on the other side to a 168µm outer diameter fused silica cannula. This cannula was chosen as it showed minimal backflow in preliminary experiments using an infusion rate of 0.33µl/minute.

Animal experiments

All animal experiments were performed according to the guidelines established by the European community and following a protocol approved by the local ethical and scientific committees on animal experiments at our institution. Female Wistar rats weighing 250-300 grams (Harlan, Horst, the Netherlands) were anesthetized by an intraperitoneal injection of 90 mg/kg ketamine and 10 mg/kg xylazine. The heads were shaved and the rats were placed in a stereotactic frame (Stoelting co., Wood Dale, IL). A midline incision was made to expose the cranium where two 0.8mm burr holes were made on either side 0.5mm anterior and 3.5mm lateral from the bregma. The tip of the infusion cannula was lowered into the corpus callosum/external capsule (3.5mm) or caudate putamen (6mm)

of the rat. 3µl or 10µl of 4% HSA in PBS containing the indicated amounts of AdGFP, AdCMVLacZ, 25µg Resovist® (SPIO, ferucarbotran, 64nm hydrodynamic diameter, Schering, Berlin, Germany), 1µl 0.4% trypan blue (molecular weight 960, Sigma, St. Louis, MO), or a combination of these were infused at a rate of 0.33µl/minute. To increase the extracellular space fraction, one group of rats received AdGFP in 10µl of a solution containing 4.2% mannitol. Five minutes after the end of infusion the cannula was removed at a rate of 0.5mm/minute. Three to four rats per group were used.

In the tumor experiments 500,000 C6 glioma cells were injected in a volume of 3µl PBS 5.5mm lateral and 0.5mm anterior to the bregma at a depth of 6mm in the external capsule. Tumors were allowed to grow for 4 days. After this period, a mixture of SPIO and trypan blue or SPIO, AdGFP and AdΔ24-CMV-GFP (10µl at 0.33µl/minute) was infused in the external capsule (bregma +0.5mm, lateral 3.5mm, 3.5mm deep).

Rats that were injected with adenovirus were sacrificed after 3 days, whereas rats that were injected with trypan blue were sacrificed directly at the end of infusion. Sacrificing the rats was performed by i.p. pentobarbital overdose (>120mg/kg). Brains were removed and snap frozen in liquid nitrogen for histochemistry and determination of GFP and β-galactosidase expression, iron and trypan blue distribution.

Determination of volumes of distribution and histochemistry

Rat brains were cut into 8µm or 30µm sections and slides were assessed for GFP expression (green filter, 445-490nm EX/ 515-575nm EM) or trypan blue fluorescence (far-red filter, 615-665nm EX/ 695-770nm EM) by imaging using the IVIS Lumina imaging system (Xenogen, Cranbury, NJ). The threshold level of GFP expression was determined to be 10% of peak GFP expression. The area of trypan blue staining was determined by the observed area of fluorescence in ImageJ with 10% of peak fluorescence set as threshold. β-Gal staining was performed according to the manufacturer's instructions (β-Gal Staining Set; Boehringer Mannheim, Almere, The Netherlands).

Iron particles were detected by imaging of Perls stained sections. Perls iron stain was done by incubating in equal parts of 2% HCl and 2% potassium ferrocyanide yielding a blue reaction product. Slides were counterstained using hematoxylin and eosin.

Volumes of distribution were determined by multiplying the calculated areas of distribution in serial slides with the interslide distances (300µm).

Statistical analysis

Differences in infection efficiency and volumes of distribution were compared by two-sided t-test. In all experiments, $p<0.05$ was considered statistically significant.

RESULTS

Albumin does not affect in vitro adenovirus infection efficiency

Because most agents used for CED are stored and delivered in solutions containing albumin we first investigated if the albumin concentration would influence infection efficiency. To this end, we subjected U-251MG glioma cells for 30 minutes to AdGFP in medium containing various concentrations of human albumin. The percentage of infected cells ranged from 5.6±0.6% (no HSA) to 3.9±0.4% (0.4% HSA). Although higher concentrations (0.4% and 4%) of HSA slightly decreased infection efficiency, the differences were neither large nor significant ($p>0.1$ for all comparisons).

Infusion of AdGFP into rat striate – gray matter

AdGFP was infused in three different doses into the corpus striatum of Wistar rats in 3µl or 10µl total volume at a rate of 0.33µl/minute (figure 1a). In all cases, the area of GFP expression was confined to the striate with minimal backflow occurring into the white matter of the external capsule.

At the two lower virus doses, the Vd achieved with the two infusion volumes (3µl and 10µl) was almost the same reaching approximately 10µl at $8.4x10^6$ iu and approximately 25µl at $8.4x10^7$ iu (figure 1b). Infusing the maximum dose that could be delivered ($2.8x10^8$ iu in 10µl) resulted in a further increase of Vd to 46.2±9.8µl, almost filling the complete striate. These results demonstrate that the distribution of AdGFP in the rat striate is dependent on the dose, rather than the infusion volume.

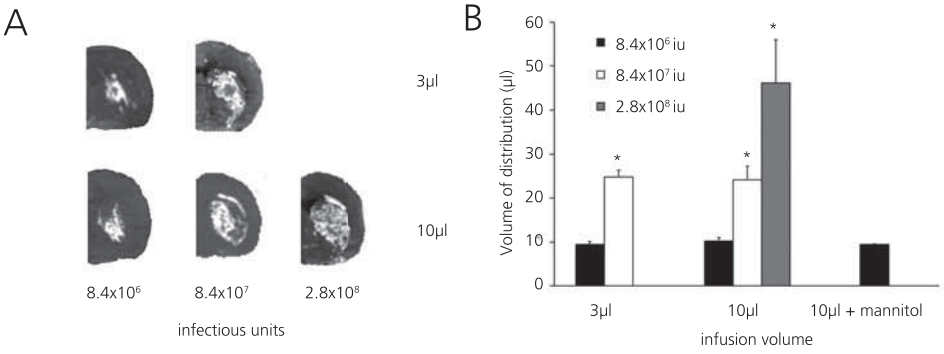

Figure 1. Volumes of distribution (Vd) of adenoviral transgene expression in rat striate. GFP expression following 3µl (left side) or 10µl infusion (right side) of AdGFP as detected by fluorescence imaging using IVIS lumina imaging system. Vd was calculated from serial slides by determining GFP expression. **A** Distribution after infusion of AdGFP in 3µl (upper) or 10µl (lower) at increasing dose as determined by IVIS fluorescence. Representative sections from rat hemispheres are shown. **B** Vd of AdGFP infused in either 3µl or 10µl with increasing dose. $8.4*10^6$ iu (black bars), $8.4*10^7$ iu (white bars) and $2.8*10^8$ iu (gray bars). Differences between 3µl and 10µl infusion volume at similar doses were not significant. Mannitol did not increase Vd. Average Vd ± SD is shown, * $p<0.01$ compared to lower dose.

In an attempt to increase the interstitial space, mannitol was co-infused but this did not change the resulting Vd (9.3±0.2µl versus 10.2±0.7µl, p>0.3; figure 1b).

Infusion of AdGFP into corpus callosum and external capsule - white matter

AdGFP was infused into the most prominent white matter tract of the rat (figure 2). In contrast to the striate, the typical anatomical orientation of the corpus callosum and the external capsule, thinning rapidly lateral from the corpus callosum, complicates objective volume measurements. Increasing the infusion volume from 3µl to 10µl increased the Vd insignificantly from 7.1±4.8µl to 9±2.5µl. More relevant however, the maximum distance traveled by the viral particles as shown by GFP expression following infusion in 10µl was on average 1.4-fold greater than following infusion in 3µl, both in the coronal (1.4±0.2, $p<0.05$) and the sagittal (1.4±0.1, $p<0.05$) plane. The maximum distance from the point of infusion traveled by the virus injected in 10µl was 6.1mm in the coronal plane and 2.4mm in the sagittal plane. These results indicate that in the white matter, the distribution of adenovirus is at least partly dependent on infusion volume.

Prediction of Adenoviral Vd by superparamagnetic iron oxide nanoparticle infusion

25µg of SPIO and $8.4x10^6$ iu adenovirus were co-infused in either 3µl or 10µl into the rat striate or external capsule. Adenovirus Vds and distribution patterns were comparable to those found when Ads were infused without SPIO and the Vds of co-infused SPIO and virus were completely overlapping (figure 3a). In the

Figure 2. Distribution of adenoviral transgene expression in rat corpus callosum and external capsule. 3µl or 10µl of AdGFP containing $8.4*10^6$ iu was infused into the external capsule. 30µm sections of one representative rat are shown. Left side of images: 3µl infusion, right side: 10µl infusion. Slides are arranged in rostrocaudal (from upper left to lower right) direction. GFP expression is extended when virus is infused in 10µl compared to bolus, both in coronal and sagittal planes.

striate, there was no increase in distribution with increasing infusion volume, while in the corpus callosum and external capsule viral spreading, as measured by the distance covered by GFP expression, increased with increasing Vi. SPIO Vds in the striate were 9.4±0.7µl and 10.8±1.1µl following 3µl and 10µl infusion, respectively, comparable to the Vd of GFP (figure 3b). In the white matter a similar relation between covered distance and infusion volume was found for SPIO and adenovirus (including a factor 1.4 difference between 3µl and 10µl). From these results it appears that 64nm SPIO and adenovirus distribute in a similar fashion through the rat brain.

Glial cell infection by adenovirus

Axonal transport of GFP, especially in the white matter, could theoretically have biased the determination of the actual Vd. As GFP is not the most sensitive marker for the determination of the type of infected cells, $8.4x10^6$ iu of Ad.LacZ was infused together with 25µg SPIO in 10µl PBS. β-galactosidase is expressed from this vector in the nuclei of infected cells, allowing for a more specific determination of the type of infected cells by nuclear morphology. Infected cells were primarily oligodendrocytes, astrocytes and other glial cell types (figure 4). No infected neurons were observed and no β-galactosidase positive cells were seen in the overlying cortex, confirming that the GFP expression seen was not due to axonal transport, but probably caused by GFP expression in the myelin sheath forming glial cells. Therefore adenovirus appeared to infect similar glial cell types in both white and gray matter. Co-infused SPIO co-localized with infected nuclei in both locations.

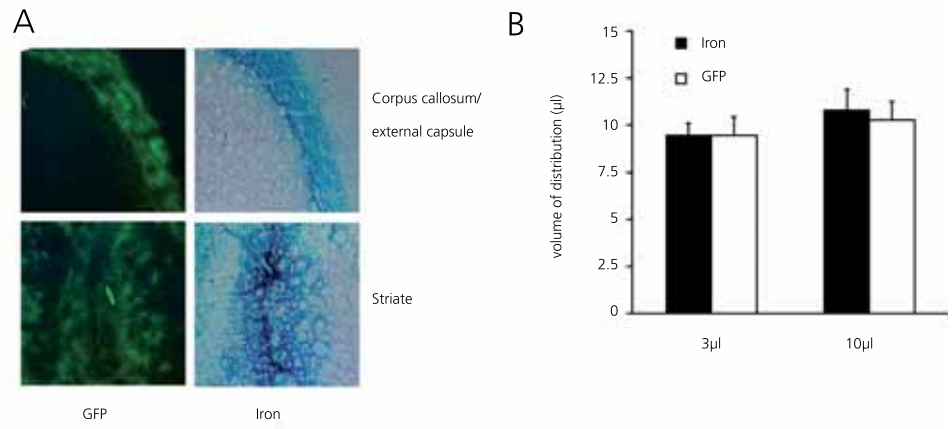

Figure 3. Co-infusion of SPIO and AdGFP in rat striate and corpus callosum. **A** Parallel 30µm coronal sections three days after infusion. GFP and HE & iron stained sections showing GFP expression in external capsule and striate (left column) and corresponding iron distribution (right column). Original magnification 5x. **B** Vd of SPIO (black bars) and AdGFP (white bars) following 3µl or 10µl infusion into rat striate combined with AdGFP. No significant differences were noted. Average Vd ± SD are shown.

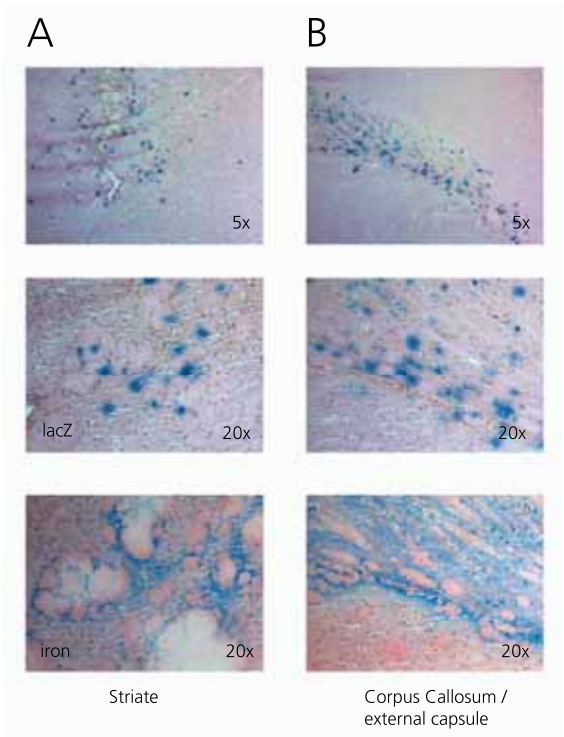

Figure 4. Determination of infected cells by nuclear morphology (top 2 rows, original magnification 5x and 20x, HE staining). β-Gal staining shows glial cells are infected following infusion of AdCMVLacZ in the rat striate (**A**) or external capsule (**B**). No infected neurons were detected. No infected cells were detected in the overlying neocortex. SPIO distribution (iron staining) is similar to β-Galactosidase staining both in gray and white matter (bottom row, original magnification 20x).

Co-infusion of SPIO and trypan blue

Adenovirus and SPIO distribution in the white matter increased with increasing volume, but not as much as would be predicted on the basis of the volume of the interstitial space (which would yield a Vd/Vi ratio of 5). We hypothesized that the effect of CED of viral particles in rat white matter might be limited by infusion fluid partly entering the gray matter, while larger particles distributed only in the white matter. To investigate this, SPIO were co-infused with trypan blue into the external capsule and rats were immediately sacrificed after infusion. As before, SPIO distributed only in the white matter of the corpus callosum and the external capsule. In contrast, trypan blue could be detected in the white matter and extending into the gray matter of both overlying neocortex and corpus striatum (figure 5a). In these particular experiments, total Vds of SPIO were 8.9±6μl (Vi=3μl, Vd/Vi ratio 3.0) and 16.9±4μl (Vi=10μl, Vd/Vi ratio 1.7). The corresponding trypan blue Vds were 18.4±5μl (Vd/Vi ratio 6.1) and 47.1±3μl (Vd/Vi ratio 4.7), showing effective trypan blue convection with a high Vd/Vi ratio close to the predicted value. This was confirmed by measuring the total fluorescence signal and average fluorescence per unit volume (figure 5b). While similar amounts of trypan blue were delivered (measured by total fluorescence), infusion in a larger volume yielded a lower fluorescence per volume due to distribution over a larger volume.

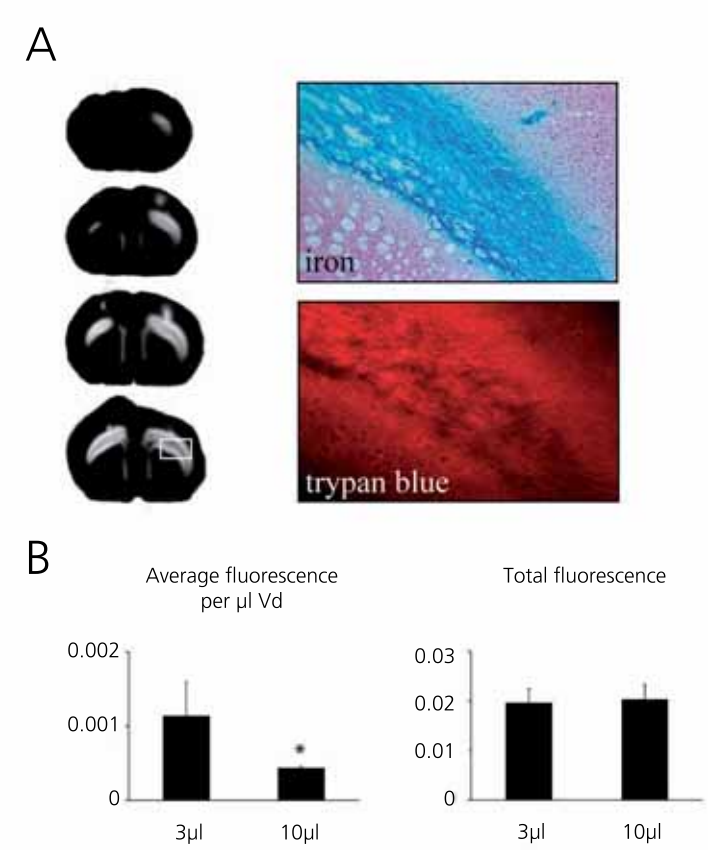

Figure 5. Determination of fluorescence of trypan blue and SPIO distribution following CED into the external capsule. Trypan blue fluorescence was detected using the IVIS Lumina system and by fluorescent microscopy. Fluorescence was quantified using ImageJ software. **A** Trypan blue is detected in the gray matter surrounding the corpus callosum, while SPIO is confined to the corpus callosum. Trypan blue is easily detected using fluorescent imaging. Both IVIS imaging (left) and microscopy fluorescence imaging (lower right panel, showing magnified view of the area marked white in left panel) yield similar distribution patterns. Image shows coronal sections through rat brain. Fluorescence signal showing in white. Right side 10µl infusion, left side 3µl infusion. Upper right panel shows corresponding HE & iron staining in parallel section, showing SPIO distribution confined to the corpus callosum and external capsule (original magnification 5x). **B** Trypan blue fluorescence used to determine if CED was successful. Average fluorescence per µl distribution volume is decreased on the 10µl side due to the larger Vd. Total fluorescence in both groups is similar indicating equal delivered dose. Average fluorescence ± SD is shown.

Targeting infiltrative tumors in the white matter.

C6 infiltrative brain tumors located in the external capsule were targeted via white matter tracts using a mixture of SPIO and trypan blue or SPIO, AdGFP and AdΔ24-CMV-GFP. The latter mixture was chosen as *in vitro* results showed that the replicating AdΔ24-CMV-GFP at 100 iu/cell provided almost a 1000-fold higher transgene expression in C6 cells when compared to AdGFP (89.7±5.3%

vs. 0.1±0.6% transduction, respectively, p<0.0001), while AdGFP showed higher levels of transgene expression in normal brain (data not shown).

Although tumor and infusion locations were several millimeters apart, directly after infusion SPIO was noted at locations where tumor cells infiltrated the white matter tracts (figure 6a). Neither iron particles nor trypan blue showed efficient penetration into solid tumor. Iron particles were noted surrounding single tumor cells, appearing to be extracellular at this stage. Three days after infusion of SPIO and adenovirus, GFP expression was seen at the rim of tumors, co-localizing with iron distribution within the solid tumor (figure 6b). Iron particles now appeared to be intracellular although no differentiation between uptake in tumor cells and reactive astrocytes could be made. Tumors that were located only just outside the white matter in the cortex were not transduced (data not shown).

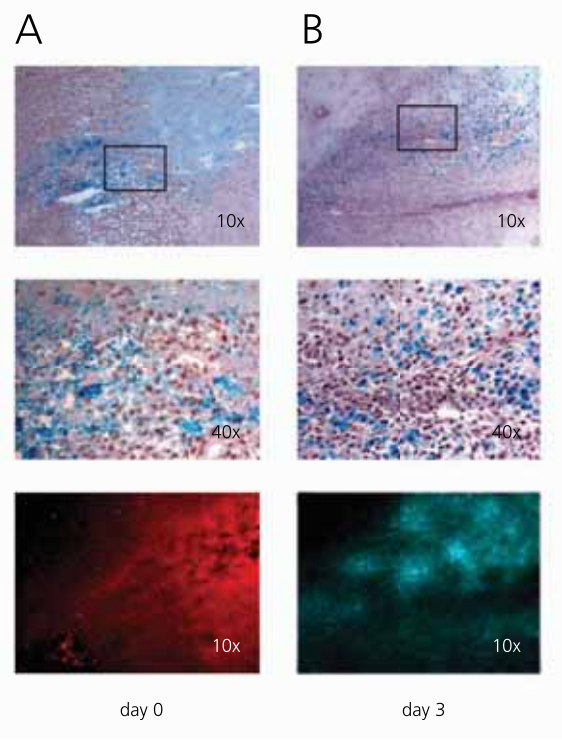

Figure 6. CED of trypan blue, SPIO and adenovirus targeting infiltrative C6 tumors. When tumor infiltrated the white matter, iron particles are seen engulfing tumor cells. Penetration into solid tumor is limited either with SPIO (top two rows), trypan blue (**A**, bottom row) or adenovirus infusion (GFP, **B**, bottom row). Bottom row trypan blue and GFP images correspond to top row Perls stained images. **A** Iron and trypan blue distribution directly after infusion. **B** Iron and GFP distribution three days after infusion.

DISCUSSION

In the current study we used a small diameter fused silica infusion cannula to convect an adenoviral vector into the rat brain and towards brain tumors. We show that while the volume of distribution is related to infused dose in the gray matter of the corpus striatum, it appears to be related to infusion volume in the white matter of the corpus callosum and external capsule. In addition we show

that the distribution of Ads is similar to that of similar sized SPIO that can thus be used to predict the distribution of adenoviruses in the brain. Finally, distant tumors can be reached by CED of adenoviruses, but penetration of these tumors is limited.

The results have some important implications for the delivery of adenoviruses in the treatment of neurologic diseases for which they have recently been used and especially for brain tumors where the migrated cells in the surrounding brain parenchyma, mainly consisting of white matter, are the target of treatment [9, 12, 22].

Because the albumin concentration of the infusion fluid had no influence on infection efficiency, a 4% albumin concentration was chosen as this concentration has been shown to increase the distribution volume of adenoviruses [16], possibly because albumin stabilizes the viral solution and prevents aggregation of viral particles [23], which could affect their distribution.

Ideally, CED of adenoviruses in a clinical setting should rely on the infused volume instead of the infused dose, as this would permit control over the desired distribution volume. Most of the recent studies using adenoviral vectors in the brain did not investigate the effect of infusion volume on the distribution of adenoviruses [16, 24-26]. One previous study that did, reported a correlation to infused dose rather than infused volume when an adenoviral vector was infused into the rat striate[14], which is similar to the results obtained from the striatal gray matter infusions in our study and other studies infusing large particles in the striate[27, 28]. These results suggest that sufficient room exists in the interstitial space of the striate for viral particles to distribute and that this distribution is not dependent upon convection, but more likely on other factors such as receptor saturation or diffusion. Because the width, or pore size, of gray matter extracellular space is estimated to be 38-64nm[29], it appears likely that adenovirus distribution in the striate does not occur in the parenchymal interstitium but along preferred routes such as perivascular spaces which have a far greater diameter (500nm) [30]. This distribution pattern has previously been observed with other large particles such as liposomes and adeno-associated viruses and is thought to be dependent on cardiac pulsations that propel the particles in the perivascular space [31-33]. The observation in our study that the Vd/Vi ratio could increase well beyond the expected value strongly suggests that such an active transport also affects adenoviral distribution and could obscure any effects from infusion driven bulk flow. In addition, the lack of an increased Vd when mannitol is co-infused to extend the interstitial space supports the concept of perivascular propagation because the perivascular spaces have sufficient space to accommodate viral transport, even without the addition of mannitol.

In the white matter of the corpus callosum and external capsule, the distribution of adenoviruses appears to be dependent on infusion volume. This was however not reflected in a substantially increased Vd. Most likely the adenoviral particle is confined to the white matter whereas the infusion fluid is not, which we

showed in the experiments co-infusing trypan blue and SPIOs with the latter exhibiting a similar distribution pattern as adenovirus. A possible explanation for the differential distribution of adenoviruses in white compared to gray matter could be related to differences in ECS composition. Both electron microscopy and mathematical analysis have shown that the white, but not the gray, matter ECS is easily extended by edema or infusion fluid [34-36], possibly enough to allow the transport of adenovirus by bulk flow. In addition, glypican, a member of the heparan sulfate proteoglycans that are known to act as co-receptors for adenovirus binding [37], is expressed in gray but not white matter of the rat [38]. Increased adenovirus binding to glypican in gray matter could also explain the limited propagation of virus particles in gray matter. Interestingly, in a study infusing Indian ink, it has been shown that this large particle (250nm) spreads diffusively through the interstitial space of white matter but was confined to the perivascular spaces in gray matter [39]. Assuming a similar distribution pattern of adenoviruses would explain why the viral particle is distributed by Vi dependent interstitial bulk flow in the white matter and by perivascular transport in the striatal gray matter.

Differential expression of transgene by neurons and glial cells could partly explain the noted transgene distributions, as neuronal cell bodies will be more abundant in gray matter. We observed no differences in transduced cell types between white and gray matter, showing only transgene expression in glial cells. Obviously, these results do not rule out the infection of neurons by adenovirus that has been observed by others [25, 40], as transgene expression may have been below detection limits. However, such a differential expression would not likely explain the differences in distribution volume when only the infusion volume is changed.

The scarcity of white matter in the rat brain compared to the abundance in the human brain raises issues on the use of this animal as a model for CED. From the current study we cannot determine if the relation between Vi and Vd in white matter is maintained when larger volumes are infused. Indeed, the larger canine brain may be better suited for preclinical evaluation of this technique [24, 25, 40]. In addition, the use of such a model would provide the possibility to study the distribution of these particles in other white matter tracts that may be clinically relevant.

Distribution patterns of SPIOs were comparable to those of adenovirus. The SPIO used, Resovist®, has a hydrodynamic diameter of 64nm, which makes it comparable, though slightly smaller, to adenovirus. Iron particles have been used to predict the distribution of adeno associated viruses (AAV) by MRI [28]. From the results of our experiments it appears that distribution of adenovirus and SPIO is very similar and since MR imaging of these agents has been shown to be feasible at a concentration of 1mg/ml [27, 28, 41], which is slightly less than the concentration used in this study, SPIO infusion could thus be considered to confirm the proper positioning of CED catheters. This strategy could be used to prevent adenoviral

distribution to undesired locations and to predict the distribution of adenoviruses following CED.

When tumors located in the white matter were targeted by infusing adenoviruses and SPIO from a distant location, we show that while the particles reach and engulf infiltrating tumor cells, infection of tumor cells or deposition of iron particles is confined to the outer rim of the solid tumor parts. Even trypan blue does not easily penetrate the solid tumor parts. In addition, when tumors were located only slightly outside the main white matter tract, no transduction of tumor cells was noticed. Factors explaining these results may be the high interstitial pressure in solid tumors and the increased tortuosity of brain tumor extracellular space limiting diffusion of particles [42-44]. In the specific case of gene therapy, these results imply that transduction of distant solid tumors using non replicating vectors will prove to be cumbersome, but that this technique might be used to reach solitary migrating tumor cells. In addition, CED of replicating (oncolytic) adenoviruses might be employed to provide a starting point for adenoviral oncolysis following infection of the rim of solid tumor parts.

In CED, catheter placement is crucial. Our results suggest that placement of catheters in the gray matter should be avoided when convecting large particles such as adenoviruses. In addition we show that CED of adenoviruses is incapable of delivering viral particles in the gray matter using white matter tracts. These factors should be considered when catheter planning is performed and could possibly be integrated into models predicting convective delivery [45].

In conclusion, the current study shows that CED of Adenoviruses is feasible when gray and white matter differences are considered and the distribution can be predicted by SPIO infusion. The observed distribution pattern of adenovirus after CED closely mimics the routes of migrating single tumor cells [46, 47], which could make CED of adenoviruses a suitable delivery method to track these cells in the treatment of gliomas.

REFERENCES

1. Bobo RH, Laske DW, Akbasak A, Morrison PF, Dedrick RL, Oldfield EH. Convection-enhanced delivery of macromolecules in the brain. ProcNatlAcadSciUSA 1994;91:2076-2080.
2. Lieberman DM, Laske DW, Morrison PF, Bankiewicz KS, Oldfield EH. Convection-enhanced distribution of large molecules in gray matter during interstitial drug infusion. JNeurosurg 1995;82:1021-1029.
3. Lonser RR, Corthesy ME, Morrison PF, Gogate N, Oldfield EH. Convection-enhanced selective excitotoxic ablation of the neurons of the globus pallidus internus for treatment of parkinsonism in nonhuman primates. JNeurosurg 1999;91:294-302.
4. Lopez KA, Waziri AE, Canoll PD, Bruce JN. Convection-enhanced delivery in the treatment of malignant glioma. NeurolRes 2006;28:542-548.
5. Kunwar S, Prados MD, Chang SM, et al. Direct intracerebral delivery of cintredekin besudotox (IL13-PE38QQR) in recurrent malignant glioma: a report by the Cintredekin Besudotox Intraparenchymal Study Group. JClinOncol 2007;25:837-844.
6. Kunwar S, Chang SM, Prados MD, et al. Safety of intraparenchymal convection-enhanced delivery of cintredekin besudotox in early-phase studies. NeurosurgFocus 2006;20:E15.
7. Sampson JH, Akabani G, Archer GE, et al. Progress report of a Phase I study of the intracerebral microinfusion of a recombinant chimeric protein composed of transforming growth factor (TGF)-alpha and a mutated form of the Pseudomonas exotoxin termed PE-38 (TP-38) for the treatment of malignant brain tumors. JNeurooncol 2003;65:27-35.
8. Sampson JH, Brady ML, Petry NA, et al. Intracerebral infusate distribution by convection-enhanced delivery in humans with malignant gliomas: descriptive effects of target anatomy and catheter positioning. Neurosurgery 2007;60:ONS89-ONS98.
9. Chiocca EA, Abbed KM, Tatter S, et al. A phase I open-label, dose-escalation, multi-institutional trial of injection with an E1B-Attenuated adenovirus, ONYX-015, into the peritumoral region of recurrent malignant gliomas, in the adjuvant setting. MolTher 2004;10:958-966.
10. Choi-Lundberg DL, Lin Q, Chang YN, et al. Dopaminergic neurons protected from degeneration by GDNF gene therapy. Science 1997;275:838-841.
11. Kirn D. Clinical research results with dl1520 (Onyx-015), a replication-selective adenovirus for the treatment of cancer: what have we learned? Gene Ther 2001;8:89-98.
12. Lang FF, Bruner JM, Fuller GN, et al. Phase I trial of adenovirus-mediated p53 gene therapy for recurrent glioma: biological and clinical results. JClinOncol 2003;21:2508-2518.
13. Puumalainen AM, Vapalahti M, Agrawal RS, et al. Beta-galactosidase gene transfer to human malignant glioma in vivo using replication-deficient retroviruses and adenoviruses. HumGene Ther 1998;9:1769-1774.
14. Betz AL, Shakui P, Davidson BL. Gene transfer to rodent brain with recombinant adenoviral vectors: effects of infusion parameters, infectious titer, and virus concentration on transduction volume. ExpNeurol 1998;150:136-142.
15. Chen MY, Lonser RR, Morrison PF, Governale LS, Oldfield EH. Variables affecting convection-enhanced delivery to the striatum: a systematic examination of rate of infusion, cannula size, infusate concentration, and tissue-cannula sealing time. JNeurosurg 1999;90:315-320.
16. Chen MY, Hoffer A, Morrison PF, et al. Surface properties, more than size, limiting convective distribution of virus-sized particles and viruses in the central nervous system. JNeurosurg 2005;103:311-319.
17. van Beusechem VW, van Rijswijk AL, van Es HH, Haisma HJ, Pinedo HM,

Gerritsen WR. Recombinant adenovirus vectors with knobless fibers for targeted gene transfer. Gene Ther 2000;7:1940-1946.

18. Grill J, Lamfers ML, van Beusechem VW, et al. The organotypic multicellular spheroid is a relevant three-dimensional model to study adenovirus replication and penetration in human tumors in vitro. MolTher 2002;6:609-614.
19. van Beusechem VW, van den Doel PB, Grill J, Pinedo HM, Gerritsen WR. Conditionally replicative adenovirus expressing p53 exhibits enhanced oncolytic potency. Cancer Res 2002;62:6165-6171.
20. Fueyo J, Gomez-Manzano C, Alemany R, et al. A mutant oncolytic adenovirus targeting the Rb pathway produces anti-glioma effect in vivo. Oncogene 2000;19:2-12.
21. Lonser RR, Gogate N, Morrison PF, Wood JD, Oldfield EH. Direct convective delivery of macromolecules to the spinal cord. JNeurosurg 1998;89:616-622.
22. Horellou P, Sabate O, Buc-Caron MH, Mallet J. Adenovirus-mediated gene transfer to the central nervous system for Parkinson's disease. ExpNeurol 1997;144:131-138.
23. Hosokawa M, Hama S, Mandai K, et al. Preparation of purified, sterilized, and stable adenovirus vectors using albumin. JVirolMethods 2002;103:191-199.
24. Oh S, Pluhar GE, McNeil EA, et al. Efficacy of nonviral gene transfer in the canine brain. JNeurosurg 2007;107:136-144.
25. Candolfi M, Kroeger KM, Pluhar GE, et al. Adenoviral-mediated gene transfer into the canine brain in vivo. Neurosurgery 2007;60:167-177.
26. Oh S, Odland R, Wilson SR, et al. Improved distribution of small molecules and viral vectors in the murine brain using a hollow fiber catheter. JNeurosurg 2007;107:568-577.
27. Kroll RA, Pagel MA, Muldoon LL, Roman-Goldstein S, Neuwelt EA. Increasing volume of distribution to the brain with interstitial infusion: dose, rather than convection, might be the most important factor. Neurosurgery 1996;38:746-752.
28. Szerlip NJ, Walbridge S, Yang L, et al. Real-time imaging of convection-enhanced delivery of viruses and virus-sized particles. JNeurosurg 2007;107:560-567.
29. Thorne RG, Nicholson C. In vivo diffusion analysis with quantum dots and dextrans predicts the width of brain extracellular space. ProcNatlAcadSciUSA 2006;103:5567-5572.
30. Huynh GH, Deen DF, Szoka FC, Jr. Barriers to carrier mediated drug and gene delivery to brain tumors. JControl Release 2006;110:236-259.
31. Mamot C, Nguyen JB, Pourdehnad M, et al. Extensive distribution of liposomes in rodent brains and brain tumors following convection-enhanced delivery. JNeurooncol 2004;68:1-9.
32. Hadaczek P, Yamashita Y, Mirek H, et al. The "perivascular pump" driven by arterial pulsation is a powerful mechanism for the distribution of therapeutic molecules within the brain. MolTher 2006;14:69-78.
33. Krauze MT, Saito R, Noble C, et al. Effects of the perivascular space on convection-enhanced delivery of liposomes in primate putamen. ExpNeurol 2005;196:104-111.
34. Kuroiwa T, Nagaoka T, Ueki M, et al. Correlations between the apparent diffusion coefficient, water content, and ultrastructure after induction of vasogenic brain edema in cats. JNeurosurg 1999;90:499-503.
35. Whittle IR, Miller JD. A rodent model of infusion brain edema: methodology and pathophysiological effects of saline and protein infusions. Acta Neurochir(Wien) 1990;105:158-168.
36. Basser PJ. Interstitial pressure, volume, and flow during infusion into brain tissue. MicrovascRes 1992;44:143-165.
37. Dechecchi MC, Tamanini A, Bonizzato A, Cabrini G. Heparan sulfate glycosaminoglycans are involved in ad-

enovirus type 5 and 2-host cell interactions. Virology 2000;268:382-390.

38. Karthikeyan L, Flad M, Engel M, Meyer-Puttlitz B, Margolis RU, Margolis RK. Immunocytochemical and in situ hybridization studies of the heparan sulfate proteoglycan, glypican, in nervous tissue. JCell Sci 1994;107 (Pt 11):3213-3222.
39. Zhang ET, Richards HK, Kida S, Weller RO. Directional and compartmentalised drainage of interstitial fluid and cerebrospinal fluid from the rat brain. Acta Neuropathol 1992;83:233-239.
40. Candolfi M, Pluhar GE, Kroeger K, et al. Optimization of adenoviral vector-mediated transgene expression in the canine brain in vivo, and in canine glioma cells in vitro. NeuroOncol 2007;9:245-258.
41. Muldoon LL, Sandor M, Pinkston KE, Neuwelt EA. Imaging, distribution, and toxicity of superparamagnetic iron oxide magnetic resonance nanoparticles in the rat brain and intracerebral tumor. Neurosurgery 2005;57:785-796.
42. Vavra M, Ali MJ, Kang EW, et al. Comparative pharmacokinetics of 14C-sucrose in RG-2 rat gliomas after intravenous and convection-enhanced delivery. Neuro-oncol 2004;6:104-112.
43. Vargova L, Homola A, Zamecnik J, Tichy M, Benes V, Sykova E. Diffusion parameters of the extracellular space in human gliomas. Glia 2003;42:77-88.
44. Zamecnik J, Vargova L, Kodet R, Sykova E. [The role of the extracellular space in biology of glial brain tumors]. CeskPatol 2005;41:12-18.
45. Sampson JH, Raghavan R, Brady ML, et al. Clinical utility of a patient-specific algorithm for simulating intracerebral drug infusions. Neuro-oncol 2007.
46. Giese A, Bjerkvig R, Berens ME, Westphal M. Cost of migration: invasion of malignant gliomas and implications for treatment. JClinOncol 2003;21:1624-1636.
47. Claes A, Idema AJ, Wesseling P. Diffuse glioma growth: a guerilla war. Acta Neuropathol(Berl) 2007;114:443-458.